

Breaking the degeneracy between polarization efficiency and cosmological parameters in CMB experiments

Silvia Galli,^{1,*} W. L. Kimmy Wu,^{2,3,†} Karim Benabed,¹ François Bouchet,¹ Thomas M. Crawford,^{3,4} and Eric Hivon¹

¹*Sorbonne Université, CNRS, Institut d’Astrophysique de Paris, 98 bis Boulevard Arago, F-75014 Paris, France*

²*SLAC National Accelerator Laboratory & KIPAC, 2575 Sand Hill Road, Menlo Park, CA 94025*

³*Kavli Institute for Cosmological Physics, University of Chicago, Chicago, Illinois 60637, U.S.A*

⁴*Department of Astronomy and Astrophysics, University of Chicago, 5640 South Ellis Avenue, Chicago, IL, 60637, USA*

(Dated: February 12, 2022)

Accurate cosmological parameter estimates using polarization data of the cosmic microwave background (CMB) put stringent requirements on map calibration, as highlighted in the recent results from the *Planck* satellite. In this paper, we point out that a model-dependent determination of polarization calibration can be achieved by the joint fit of the TE and EE CMB power spectra. This provides a valuable cross-check to band-averaged polarization efficiency measurements determined using other approaches. We demonstrate that, in Λ CDM, the combination of the TE and EE constrain polarization calibration with sub-percent uncertainty with *Planck* data and 2% uncertainty with SPTPOL data. We arrive at similar conclusions when extending Λ CDM to include the amplitude of lensing A_L , the number of relativistic species N_{eff} , or the sum of the neutrino masses $\sum m_\nu$. The uncertainties on cosmological parameters are minimally impacted when marginalizing over polarization calibration, except, as can be expected, for the uncertainty on the amplitude of the primordial scalar power spectrum $\ln(10^{10}A_s)$, which increases by 20 – 50%. However, this information can be fully recovered by adding TT data. For current and future ground-based experiments, SPT-3G and CMB-S4, we forecast the cosmological parameter uncertainties to be minimally degraded when marginalizing over polarization calibration parameters. In addition, CMB-S4 could constrain its polarization calibration at the level of $\sim 0.2\%$ by combining TE and EE, and reach $\sim 0.06\%$ by also including TT. We therefore conclude that relying on calibrating against *Planck* polarization maps, whose statistical uncertainty is limited to $\sim 0.5\%$, would be insufficient for upcoming experiments.

I. INTRODUCTION

The Λ cold dark matter (Λ CDM) model has emerged to be the leading model in describing our universe since the advent of precision measurements of the anisotropies in the cosmic microwave background (CMB). On the largest angular scales, we have satellite measurements from WMAP and *Planck* that reach cosmic-variance limits in the temperature anisotropy spectrum up to multipoles $\ell \sim 500$ and $\ell \sim 1600$ respectively [1–3]. On small angular scales, large aperture ground-based experiments like the Atacama Cosmology Telescope (ACT) and the South Pole Telescope (SPT) provide high signal-to-noise measurements of the CMB damping tail [4, 5], in both temperature and polarization.

As elucidated and forecasted in [6] and demonstrated by *Planck* and recent results from ground-based telescopes, polarization measurements of the CMB are increasingly dominating over the temperature measurements in terms of their statistical constraining power on cosmological parameters. However, in order to fully take advantage of these upcoming data sets, systematic errors that could bias the polarization measurements must be sufficiently mitigated and controlled. Specifically, recent *Planck* results show that cosmological parameters can be biased by one of the main polarization systematics—errors in the estimates of the polarization efficiencies of the detectors [7, 8]. For *Planck*, the polarization efficiencies of its detectors as measured in-flight were

discrepant from what were expected from laboratory measurements by up to 5 times the statistical uncertainties of the laboratory measurements [9]. To account for this discrepancy, the *Planck* polarization calibrations at different frequencies were then re-evaluated by requiring the polarization spectra to recover the Λ CDM cosmology inferred by the temperature spectrum measurements, effectively modeling the detector polarization efficiencies as overall calibration of the polarization maps per frequency, P_{cal} .

In this work, we propose an alternative method to extract polarization calibration as a potential cross-check for direct approaches. Typically, polarization calibration parameters are included in cosmological parameter estimation as nuisance parameters with priors informed by external calibration steps [e.g. 10–12]. Here, we jointly fit the Λ CDM and extension models to the CMB TE and EE spectra allowing the polarization calibration parameters to float, i.e., we let the data to self-calibrate P_{cal} given a model. We show that the combination of just TE and EE is sufficient in providing a tight P_{cal} constraint, and the P_{cal} uncertainty can be further improved by including the temperature power spectrum TT. Atmospheric noise degrades the ground-based TT measurement more than satellite TT or ground-based TE and EE measurements. For this reason, the ability to self-calibrate P_{cal} with only TE and EE as demonstrated by this work is of particular interest to current and upcoming ground-based experiments [e.g. 13–17].

The inferred polarization calibration from our proposed method can produce tight constraints because of the different dependence on P_{cal} of TE and EE, which breaks parameter degeneracies with other cosmological parameters. While this inferred polarization calibration is admittedly model-dependent,

* galli@iap.fr

† wlwu@slac.stanford.edu

it is nevertheless useful as a consistency check against polarization calibration estimated through other methods. Furthermore, we show that most Λ CDM parameter constraints are only mildly to negligibly degraded when marginalizing over P_{cal} , and common extensions to Λ CDM are insensitive to marginalizing over this extra parameter.

In the following, we apply this method to SPT_{POL} and *Planck* data and show that P_{cal} are constrained to percent level precision for these experiments across Λ CDM and its extensions, including the lensing amplitude A_L , the effective number of relativistic species N_{eff} , and the sum of neutrino masses $\sum m_\nu$. We take inputs from a recent SPT_{POL} power spectrum analysis [18, hereafter H18] and *Planck*'s latest data release [19] and sample parameter spaces without imposing priors on their respective polarization calibration parameters. With the recent release of the ACTpol DR4 data, we apply this method to the publicly available ACTpol_{lite} likelihood [20, 27] to demonstrate the ease of application of this approach. We use CosmoMC [21] for sampling the posterior distributions of SPT_{POL} and *Planck*, and COBAYA [22] for ACTpol. To check the relevance of this method for upcoming and future data sets, we forecast the P_{cal} uncertainty and the changes in cosmological parameter uncertainties when marginalizing over P_{cal} for SPT-3G and CMB-S4. While this paper was in its final stages of preparation, the results from the first season of the SPT-3G experiment were released [23]. We leave the application of our method to this data set to future work.

This paper is organized as follows. In Sec. II, we summarize polarization calibration as defined in SPT_{POL} and *Planck*. We present results for SPT_{POL}, ACTpol, and *Planck* in Sections III to V. Our forecasts for SPT-3G and CMB-S4 are detailed in Sec. VI. We conclude in Sec. VII.

II. POLARIZATION EFFICIENCY AND EFFECTIVE CALIBRATION

The power absorbed by a polarized detector in an experiment such as *Planck* or SPT_{POL} at time t can be modeled as:

$$P(t) = G \{ I + \rho [Q \cos 2(\psi(t)) + U \sin 2(\psi(t))] \} + n(t), \quad (1)$$

where I , Q , and U are the Stokes parameters that characterize the intensity and polarization fields, G is the effective gain (setting the absolute calibration), ρ is the detector polarization efficiency, $\psi(t)$ is the angle of the detector with respect to the sky and $n(t)$ is the detector noise. Here we have omitted effects from beams and bandpasses without loss of generality.

Intensity and polarization I , Q , and U maps per frequency are then produced via map-making [e.g., 9] by co-adding observations at different times and from different detectors. Relative calibration corrections are applied across detectors and the co-addition is weighted given the noise of the time-ordered data over some observing period. In the following, we focus on the impact of errors in the estimate of detector polarization efficiency at the coadded map level, which can be effectively captured at each frequency by a polarization calibration cor-

rection parameter P_{cal} .¹

For the SPT_{POL} TE and EE analysis in H18, polarization maps are first made incorporating detector polarization efficiencies and angles measured on ground. Then, before forming data power spectra, the temperature and polarization maps are calibrated against *Planck* maps. The calibration factors ϵ are formed by first taking the ratio of the cross-spectrum between two halves of SPT_{POL} maps and the cross-spectrum between *Planck* maps and SPT_{POL} maps. The *Planck* maps are masked and filtered identically as the SPT_{POL} maps and thus have the same filter transfer function and mode-coupling. The remaining differences from the beams B_b and the pixel-window function $\sqrt{F_b}$ of the input *Planck* maps are accounted for as follows:

$$\epsilon_b = \frac{\sqrt{F_b^{\text{Planck}}} B_b^{\text{Planck}} C_b^{\text{SPT}_i \times \text{SPT}_j}}{B_b^{\text{SPT}} C_b^{\text{SPT} \times \text{Planck}}}, \quad (2)$$

where subscript b denotes binned multipole, and i, j denote different halves of the SPT_{POL} data. The calibration factors are extracted by averaging across the multipole ranges $600 < \ell < 1000$ for temperature and $500 < \ell < 1500$ for polarization. The *Planck* DR2 Commander polarization maps are used to obtain the polarization calibration factor, and provide a $\sim 6\%$ correction to the Q and U maps (see sections 4.5.2 and 7.3 in H18 for further details). The uncertainties of the calibration factors are incorporated when sampling cosmological and nuisance parameters. Specifically, the theoretical spectra to which the data are compared are scaled by $1/(T_{\text{cal}}^2 P_{\text{cal}})$ for TE and $1/(T_{\text{cal}} P_{\text{cal}})^2$ for EE, where T_{cal} denotes the overall residual calibration of the maps and P_{cal} denotes the polarization calibration correction. Gaussian priors with mean of unity and uncertainties of 0.34% and 1% are applied to T_{cal} and P_{cal} respectively, based on the uncertainties of the ratio estimates in Eq. 2. It is the prior on P_{cal} that we remove in this work.

For *Planck*, the modeling of polarization calibration is different from the one used in H18 in two ways. First, the *Planck* likelihood at high- ℓ^2 includes maps from 3 frequencies, 100, 143, and 217 GHz, in contrast to the single-frequency analysis done in H18 at 150 GHz. Second, while the SPT_{POL} P_{cal} is defined at the map level, the *Planck* effective polarization calibration parameters c_v^{EE} are defined at the power spectrum level for each frequency spectrum $\nu \times \nu$ used in the high- ℓ likelihood.³ Thus, $P_{\text{cal}} = \sqrt{c^{EE}}$ for each frequency.

¹The polarization calibration correction parameter, P_{cal} , are sometimes called polarization efficiency corrections in *Planck* papers. Unless specifically referring to detector polarization efficiencies, we use polarization calibration P_{cal} as applied at the map level to refer to this correction. In this paper, we would often shorten ‘‘polarization calibration correction parameter’’ to polarization calibration.

²The high- ℓ likelihood covers $\ell > 30$. We assume here that polarization efficiency corrections have a negligible impact on the low- ℓ polarization likelihood due to the large uncertainties in this regime due to a combination of cosmic variance, noise, and systematic uncertainties.

³Thus, the polarization efficiency for a cross-frequency spectrum $\nu \times \nu'$ in, e.g., EE is $\sqrt{c_v^{EE} \times c_{\nu'}^{EE}}$.

Specifically, the theory power spectra to which the data is compared are multiplied by a calibration factor g defined as

$$g_{\nu \times \nu'}^{XY} = \frac{1}{2y_P^2} \left(\frac{1}{\sqrt{c_{\nu}^{XX} c_{\nu'}^{YY}}} + \frac{1}{\sqrt{c_{\nu'}^{XX} c_{\nu}^{YY}}} \right). \quad (3)$$

Here, $\nu \times \nu'$ indicate the frequency spectra with $\nu, \nu' = 100, 143, 217$ GHz; the spectra are then either for $XY = TE$ or $XY = EE$. c_{ν}^{TT} denotes temperature calibration parameters, which are separately determined and on which priors are set. c_{143}^{TT} is set to unity so that the 143 GHz temperature map is taken as a reference. Finally, y_P is the overall *Planck* calibration parameter defined at the map level, on which a Gaussian prior⁴ of $y_P = (1, 0.0025^2)$ is set (see Section 3.3.4 of [7] for further details). As detailed in Sec. V, in the baseline *Planck* analysis, c_{ν}^{EE} are fixed to the values obtained by comparing the EE data spectra to the theory spectra computed given the best-fit cosmology to the TT spectra. In this work, c_{ν}^{EE} are nuisance parameters to be constrained by the data themselves. Given the different definitions of the polarization calibration in these SPTPOL and *Planck* works, in the rest of this paper we will always specify whether the quoted uncertainties refer to the map-level (P_{cal}) or power-spectrum level (c_{ν}^{EE}) corrections. In Sec. V, we will provide results for the *Planck* data using both definitions.

III. SPTPOL

A. Data and model description

We use the SPTPOL TE and EE power spectrum measurements from H18. The generation of these measurements is described in detail in H18 and here we highlight relevant aspects of that work. Data in H18 came from the 150 GHz band observations made by the SPTPOL camera on the South Pole Telescope over an effective area of 490 deg². The power spectra cover angular multipoles ℓ between 50 and 8000. The polarization noise level measured in the range $1000 < \ell < 3000$ of this data set is 9.4 $\mu\text{K arcmin}$.

For the ΛCDM baseline case, we sample the identical model space as in H18 using the same covariance matrix with CosmoMC [21]. The model parameter space is composed of ΛCDM , foreground, and nuisance parameters. The ΛCDM parameters are the cold dark matter density $\Omega_c h^2$; the baryon density $\Omega_b h^2$; the amplitude and tilt of the primordial scalar power spectrum $\ln(10^{10} A_s)$ and n_s ; the optical depth to reionization τ ; CosmoMC's internal proxy to the angular scale of the sound horizon at decoupling, θ_{MC} . A Gaussian prior is set on τ : $(0.0544, 0.0073^2)$ given the *Planck* results [24]. The sum of neutrino mass $\sum m_{\nu}$, when not sampled, is fixed to 0.06 eV. On the other cosmological parameters, we set large uniform priors.

We consider Galactic dust foregrounds and the extragalactic foregrounds from polarized point sources. We model and set priors for them identically as in H18. The priors on the amplitudes of dust at ℓ of 80, A_{80}^{TE} and A_{80}^{EE} , are set to be uniform with $[0, 2\mu\text{K}^2]$; the priors on the spatial spectral indices, α_{TE} and α_{EE} , are set to $(-2.42, 0.02^2)$. Finally, the prior on the amplitude of polarized sources D_{3000}^{PSEE} is set to $[0, 2.5\mu\text{K}^2]$.

As in H18, the nuisance parameters are beam uncertainties, super-sample lensing [25], and temperature and polarization calibrations. We include effects from super-sample lensing with the prior on κ to be $(0.0, 0.001^2)$. We model beam uncertainties using two eigenmodes with prior $(0.0, 1^2)$ on each mode. The overall residual calibration parameter T_{cal} has prior $(1.0, 0.0034^2)$. Finally, as for the focus of this paper P_{cal} , we either set a prior of $(1.0, 0.01^2)$, which is the baseline of H18, or no prior, which is the method we propose to let P_{cal} be determined by the data.

In the following, we will report results obtained either from TE and EE separately, or from the combination of the two, which we will refer to as TE,EE.

B. Main results

To illustrate the idea, in Fig. 1, we show the 2D posterior of $\ln(10^{10} A_s)$ and P_{cal} from TE, EE, and TE,EE without imposing a P_{cal} prior. We see that without a P_{cal} prior, the constraints on A_s from TE alone and EE alone are very degenerate with P_{cal} . However, since the P_{cal} dependence from TE and EE are different (linear versus quadratic in P_{cal} respectively), the combined TE,EE constraint on A_s and P_{cal} without a prior are significantly reduced. This illustrates the potential of combining the TE and EE spectra in constraining P_{cal} without significantly degrading constraints on ΛCDM parameters. Furthermore, we find that the P_{cal} parameter as sampled is consistent with unity. This serves as cross-check to the polarization calibration determined by the comparison to the *Planck* Commander polarization maps. In the following, we first show that the constraints on P_{cal} are sufficiently precise and stable across different models to be used as a cross-check for other sources of measurements. We then discuss effects on cosmological parameter uncertainties when marginalizing over P_{cal} .

For this SPTPOL data set, we obtain a $\sim 2\%$ constraint on P_{cal} in ΛCDM and three extensions— A_L , N_{eff} , and $\sum m_{\nu}$, as listed in Tab. I and shown in Fig. 2. This level of precision is sufficient to cross-check the baseline approach used in H18 in which the SPTPOL polarization maps are calibrated against the *Planck* Commander maps. In other words, without applying the polarization calibration correction from comparing against *Planck*, one would arrive at a similar conclusion that a 6% correction should be applied to the calibration of the polarization maps if one lets P_{cal} float while sampling the ΛCDM and extension model spaces with the TE,EE data set. We note that in all three extension scenarios, the P_{cal} constraint does not degrade significantly, which shows that this approach is useful as cross-checks beyond just the ΛCDM model.

The stable uncertainties on P_{cal} across ΛCDM and the few

⁴We denote Gaussian priors with mean μ and standard deviation σ as (μ, σ^2) , and uniform priors between ν_{min} and ν_{max} as $[\nu_{\text{min}}, \nu_{\text{max}}]$.

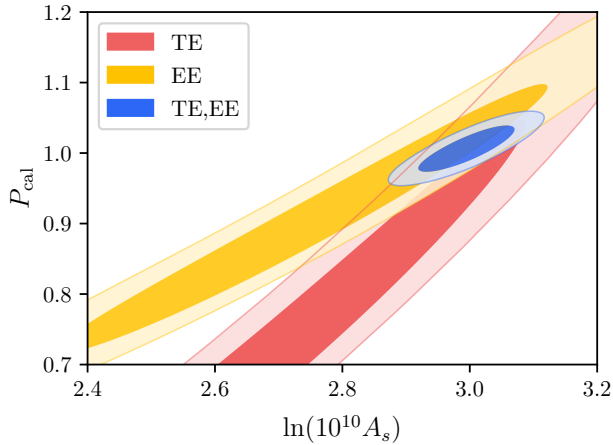


FIG. 1. $\ln(10^{10}A_s)$ vs P_{cal} in ΛCDM for SPTPOL TE, EE, and TE,EE, with no P_{cal} priors. We exploit the different degeneracy directions between $\ln(10^{10}A_s)$ and P_{cal} from TE and EE to constrain P_{cal} .

TABLE I. Polarization calibration parameters obtained from SPTPOL data assuming different models. For reference, using the baseline P_{cal} prior in H18 of 1%, we find $P_{\text{cal}} = 1.0015 \pm 0.0090$ for the ΛCDM model.

Model	SPTPOL TE,EE (no P_{cal} prior)
ΛCDM	1.0061 ± 0.0210
$\Lambda\text{CDM}+A_L$	0.9980 ± 0.0216
$\Lambda\text{CDM}+N_{\text{eff}}$	1.0126 ± 0.0222
$\Lambda\text{CDM}+\Sigma m_\nu$	1.0022 ± 0.0209

extensions suggest that P_{cal} has little degeneracy with other parameters. Indeed, most cosmological parameter constraints are only negligibly to mildly degraded when we relax the P_{cal} prior for the SPTPOL TE,EE data set. We show in Fig. 3 the ratios of cosmological parameter uncertainties between the no P_{cal} prior and the baseline P_{cal} prior case for the models considered. The constraints on A_s degrade most, by 40 – 60% depending on the model. This is expected given the correlation

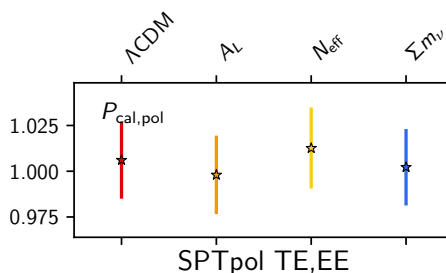


FIG. 2. Marginal mean and 68% confidence level error bars on P_{cal} obtained from SPTPOL TE,EE data assuming the ΛCDM model and a few of its extensions. The determination of P_{cal} is only slightly affected by the choice of cosmological model.

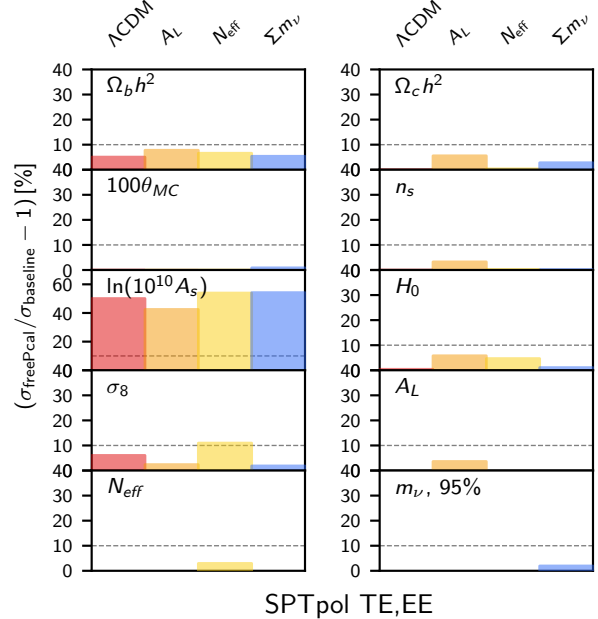


FIG. 3. Impact of freeing P_{cal} on the error bars of cosmological parameters for the SPTPOL TE,EE data. We show the ratio of the error bars obtained letting the P_{cal} parameter free to vary, over the ones obtained using the baseline SPTPOL settings, in units of percent, $\sigma_{\text{free } P_{\text{cal}}} / \sigma_{\text{baseline}} - 1$ [%]. The horizontal dashed line indicates a 10% increase in the error bars. We show results for the ΛCDM model and a few of its extensions. Only the constraints on $\ln(10^{10}A_s)$ are significantly weakened by letting P_{cal} free to vary.

between $\ln(10^{10}A_s)$ and P_{cal} . The correlation⁵ is 84% for the ΛCDM case, as suggested in Fig. 1. All of the rest of the parameter uncertainties increase by $\leq 10\%$ when marginalizing over the broadened P_{cal} posterior space. We show in Sec. VI that the degradation in A_s disappears if we include the temperature spectrum measurement TT as part of the input. This is because TT tightly constrains A_s independent of P_{cal} . For data sets similar to SPTPOL, not only are the constraints on P_{cal} precise enough for cross-checks with other approaches, most cosmological parameter constraints are also minimally degraded when no P_{cal} priors are imposed.

As one way of demonstrating consistency, we compare the inferred P_{cal} values from the TE-only and EE-only data sets when the rest of the parameters are fixed to the best-fit from the TE,EE joint fit in ΛCDM with the baseline P_{cal} prior. The marginalized P_{cal} are $P_{\text{cal}} = 0.997 \pm 0.020$ and $P_{\text{cal}} = 0.991 \pm 0.005$ for the TE and the EE data set respectively. This shows that the individual data set does not prefer a statistically different P_{cal} ; there is no significant systematic residuals that project onto P_{cal} .

⁵We define the correlation between two parameters x, y as $\rho_{xy} = \text{cov}(x, y) / \sqrt{\text{cov}(x, x)\text{cov}(y, y)}$, with $\text{cov}(x, y)$ the elements of the parameter covariance matrix.

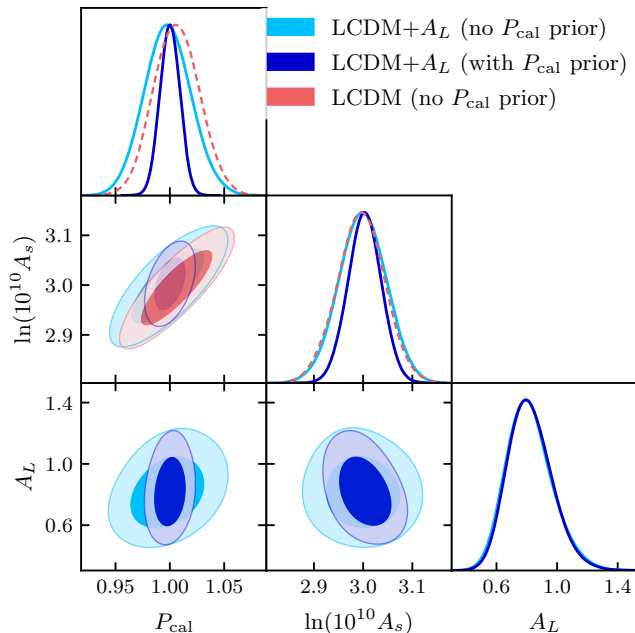


FIG. 4. A_s , P_{cal} , and A_L posteriors with and without A_L free for the SPTpol TE,EE data set. The uncertainty on A_L is unchanged with and without the P_{cal} prior, ensuring the strong A_L constraint from polarization-only spectra even when freeing P_{cal} .

C. The A_L case

We now turn to one particularly interesting parameter extension, A_L , a non-physical parameter that tunes the effect of gravitational lensing on the CMB primary spectra, changing the amount of smoothing of its peaks and troughs [26]. In *Planck*, an excess peak smoothing was observed in their temperature power spectrum at the 2.8σ level compared with the Λ CDM expectation [24]. One key way of differentiating whether the excess smoothing is a statistical fluctuation, the result of unmodeled systematic errors, or new physics is to test if this trend persists in polarization [e.g. 20]. One concern of our method would be that marginalizing over the no-prior P_{cal} would degrade the A_L constraint enough that one can no longer tell if the polarization data show similar trends. As shown in Fig. 4, the constraints on A_L for TE,EE with and without P_{cal} priors are almost identical, retiring related concerns.

As an aside, we note that the lensing information from peak smoothing reduces what would otherwise be almost complete degeneracy between P_{cal} and A_s in the TE-only and EE-only cases. Specifically, because peak smoothing provides a second handle for measuring A_s , the Λ CDM TE-only and EE-only constraints on P_{cal} are 21% and 13% respectively (as shown in the red and yellow contours in Fig. 1). By contrast, when the peak-smoothing information is absorbed by the additional parameter A_L , the P_{cal} constraints degrade by more than a factor of two in both TE-only and EE-only cases.

IV. ACTPOL

We apply this method to the recent ACTpol DR4 data set on the frequency-combined CMB-only spectra, using the ACTPOLlite likelihood [20, 27]. We note that the flat prior applied on y^P , the ACTpol polarization calibration parameter, is sufficiently broad ([0.9, 1.1]) that it is already allowing y^P to float to that extent. Here we estimate how well this ACTpol data set can constrain polarization calibration using just the TE and EE spectra, with the prior on y^P further widened. We also check if the TE,EE y^P result is consistent with the TT,TE,EE y^P result.

We use only the TE and EE frequency-combined spectra without TT on both the wide and the deep patch. We then transform the y^P samples by applying an inverse to match the P_{cal} definition, $P_{\text{cal}} = 1/y^P$. With this setup, we find $P_{\text{cal}} = 1.0113 \pm 0.0150$ in the Λ CDM model. It is consistent with the y^P result from [20], which includes the TT spectra, of $y^P = 1.0008 \pm 0.0047$.

V. PLANCK

A. Data and model description

In this section, we test whether jointly fitting the *Planck* TE and EE spectra with no prior on P_{cal} would produce sufficiently precise P_{cal} measurements to serve as useful cross-checks for other approaches. We also test the level of impact of this approach on the uncertainties on cosmological parameters.

In *Planck*, polarization efficiencies, as well as polarization angles, were measured on the ground in [28] and taken into account in the map-making algorithm SR011 [9]. At the frequencies used in the high-multipole likelihood (100, 143, 217 GHz), polarization efficiencies per detector were found to be between 83% and 96%, with estimated uncertainties between 0.1 and 0.3% at the map level. However, tests performed on the maps, which compared strongly emitting polarized galactic dust regions as observed by different detectors, suggested that residual polarization efficiency errors are several times larger than the expected uncertainties reported in [28], as shown in [9]. Left uncorrected, these residuals in the polarization efficiencies can impact cosmological parameters up to fractions of a sigma by biasing the overall amplitude of the TE and EE spectra used in the high-multipole likelihood.

In order to correct for this effect, effective polarization calibrations were estimated by the *Planck* collaboration by comparing the TE and EE power spectra at 100, 143, and 217 GHz to fiducial TE and EE spectra computed from the Λ CDM best-fit to the TT data. Polarized galactic contamination was cleaned using information from the 353 GHz channel [7]. The fits were performed on a limited range of multipoles ($\ell = 200 - 1000$) to discard regions affected by foreground cleaning or noise uncertainties and over about $\sim 60\%$ of the sky (see [7] for details). The advantage of this method is that it provides an absolute reference with small uncertainties.

The disadvantage is that the polarization efficiency corrections found in this way depend on the cosmological model fitted to the temperature data (although this was tested to have a small impact). This method enabled determinations of the polarization calibration for EE with uncertainties below $\lesssim 0.5\%$ at the map level ($\lesssim 1\%$ at power spectrum level) and for TE with uncertainties below $\lesssim 1\%$ ($\lesssim 2\%$) in each of the three frequencies used in the high-multipole *Planck* likelihood. Up to a global polarization calibration, the derived c_v^{EE} s were found to be consistent with the results of the component separation algorithm SMICA [9], which measures relative inter-frequency calibration ratios between foreground-cleaned polarization maps. Furthermore, in [7], it was noted that the estimates obtained separately from EE and TE should agree given the same polarization maps. However, the two measurements were found to differ by up to $1.7 \pm 1\%$ at the map level at 143 GHz (see Section 3.3.4 of [7]). As we will show below, this difference cannot be reconciled by the approach we propose in this work—leaving polarization efficiencies to freely vary. Since the difference in polarization calibration from TE and EE is small enough that it could be caused by statistical fluctuations, we leave the investigation of potential biases to parameters to future work and focus on the constraints on P_{cal} given the *Planck* data set and impact on cosmological parameters.

We consider the 2018 final release of the *Planck* data [7]. We use the low-multipole likelihood in polarization SimAll ($\ell = 2 - 29$ in EE only), which we will refer to as “lowE.” For high multipoles, we use the `Planck` likelihood ($\ell = 30 - 1997$ in EE and TE), which we will refer to as TE and EE separately or TE,EE when used in combination. For cross-checks, we use the `TT Commander` likelihood at low- ℓ ($\ell = 2 - 29$) and `Planck` at high- ℓ ($\ell = 30 - 2508$) and we refer to the combination of the two as TT. We model polarization calibration only for the high- ℓ likelihoods, because their impact on low- ℓ spectra are negligible compared to cosmic variance, noise, and systematic uncertainties in this multipole range. In the baseline *Planck* results using the `Planck` likelihood, the polarization calibration to the TE and EE spectra are fixed to the ones obtained from comparing the EE spectra at different frequencies to the Λ CDM best-fit of the TT+lowE data combination. These baseline parameters are listed in Table II.

B. Main results and robustness assessment

We first discuss the uncertainties on P_{cal} for the *Planck* data set when it is free to vary. Using TE,EE+lowE, we find one can determine the polarization calibrations with uncertainties smaller than $\sim 1\%$ at the map level. More specifically we find uncertainties of 0.65%, 0.6% and 0.8% at the map level for $\nu = 100, 143, 217$ GHz respectively (corresponding to 1.3%, 1.2% and 1.7% at the power spectrum level). Furthermore, we compare these uncertainties to the ones obtained with the TT power spectra included. We find that the error bars shrink by almost a factor of 2 to 0.35%, 0.31% and 0.51% at the map level for the three frequencies and similarly at the power-spectrum level. The measurements and uncertainties are re-

TABLE II. Polarization calibrations at power spectrum level obtained from *Planck* data assuming different cosmological models. We also report the corresponding polarization calibrations at map level ($P_{\text{cal}} = \sqrt{c^{EE}}, \sigma(P_{\text{cal}}) \sim (c^{EE})^{-1.5} \sigma(c^{EE})/2$), to ease the comparison with those obtained for SPT in Section III. The column “baseline” lists the fixed values used in the baseline *Planck* likelihood, which were determined with an uncertainty of $\sim 1\%$ at the power-spectrum level ($\sim 0.5\%$ at the map level).

Parameter	<i>Planck</i> TE, EE+lowE	<i>Planck</i> TT,TE, EE+lowE	baseline
ΛCDM			
C_{EE100}	0.985 ± 0.013	1.007 ± 0.007	1.021
C_{EE143}	0.954 ± 0.012	0.973 ± 0.006	0.966
C_{EE217}	1.036 ± 0.017	1.056 ± 0.011	1.04
P_{cal}^{EE100}	0.9925 ± 0.0066	1.0035 ± 0.0035	
P_{cal}^{EE143}	0.9767 ± 0.0064	0.9864 ± 0.0031	
P_{cal}^{EE217}	1.0178 ± 0.0081	1.0276 ± 0.0051	
ΛCDM+A_L			
C_{EE100}	0.989 ± 0.014	1.005 ± 0.0074	
C_{EE143}	0.957 ± 0.013	0.971 ± 0.0060	
C_{EE217}	1.040 ± 0.017	1.050 ± 0.012	
P_{cal}^{EE100}	0.9945 ± 0.0071	1.0025 ± 0.0037	
P_{cal}^{EE143}	0.9783 ± 0.0069	0.9854 ± 0.0031	
P_{cal}^{EE217}	1.0198 ± 0.0080	1.0247 ± 0.0056	
ΛCDM+N_{eff}			
C_{EE100}	0.983 ± 0.013	1.006 ± 0.0080	
C_{EE143}	0.957 ± 0.012	0.973 ± 0.0064	
C_{EE217}	1.040 ± 0.016	1.054 ± 0.012	
P_{cal}^{EE100}	0.9915 ± 0.0067	1.0030 ± 0.0040	
P_{cal}^{EE143}	0.9783 ± 0.0064	0.9864 ± 0.0033	
P_{cal}^{EE217}	1.0198 ± 0.0075	1.0266 ± 0.0055	

ported in Tab. II and shown in Fig. 5. With and without TT, the uncertainties on the P_{cal} factors are comparable to ones used in the `Planck` likelihood. This demonstrates that this approach yields relevant constraints on P_{cal} for cross-checks of other approaches.

In Tab. II, we observe shifts in the mean values of the polarization calibrations when TT are added to TE and EE. To check that the shifts are consistent with statistical fluctuations, we employ the formalism described in [29], which is applicable for comparing two data sets in which one is a subset of the other. We find that the observed shifts are consistent with statistical fluctuations at better than the $2\sigma_{\text{exp}}$ level, with $\sigma_{\text{exp}} = \sqrt{\sigma_{\text{TE,EE}}^2 - \sigma_{\text{TT,TE,EE}}^2}$. Finally, we note that the mean values recovered from the TT,TE,EE combination are slightly different from the ones used in the baseline because of statistical fluctuations due to the different multipole range and sky mask used in the two cases (see also the discussion in section 3.7 of [7]).

We further check how much the constraints degrade when we exclude the cross-frequency spectra and only use the combination of the TE and EE frequency auto-spectra 100×100 , 143×143 , and 217×217 GHz. We find in this case comparable constraints on polarization calibrations to our baseline results. Furthermore, if we include TE and EE from only one frequency instead of all three as in our previous cases, i.e., we use only the 100×100 , 143×143 , or 217×217 GHz

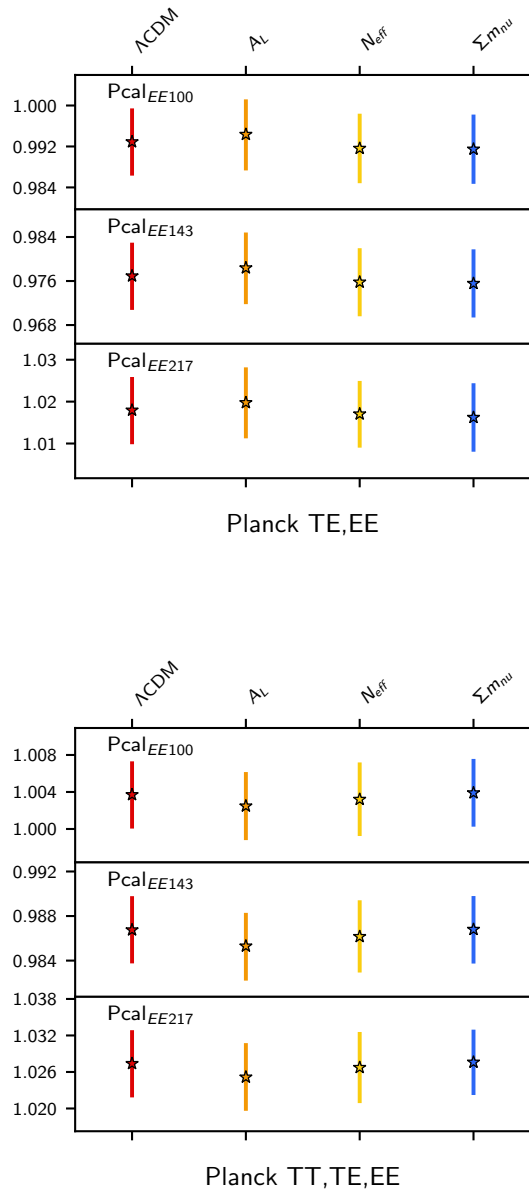


FIG. 5. Marginal mean and 68% confidence level error bars on the three *Planck* P_{cal} frequency parameters when they are let free to vary assuming different cosmological models. The top plot shows the results for *Planck* TE,EE, while the bottom one shows *Planck* TT,TE,EE. Estimates on the P_{cal} parameters do not change significantly when varying the cosmological model.

power spectra, the uncertainties of the polarization calibrations worsen to 1.1%, 0.75% and 2.1% at the map level (2.1%, 1.5% and 4.1% at the power spectrum level) respectively. The large increase in uncertainty for the 217×217 GHz case is because of the more restrictive ℓ range of 500–1996 used at this frequency, which increases the degeneracies between cosmo-

logical parameters and polarization calibrations. For the other frequencies, the degradation of the constraint is smaller than a factor of 2.

Fig. 6 shows the degeneracies between the P_{cal} parameters at different frequencies and the most degenerate cosmological parameter, $\ln(10^{10}A_s)$. When using TE,EE+lowE, $\ln(10^{10}A_s)$ has a $\sim 40\%$ correlation with each of the three P_{cal} parameters. The second most degenerate parameter is $\Omega_b h^2$ ($\sim 30\%$ correlation), while all other parameters have smaller correlations. As can be expected, we also find the degeneracies amongst the P_{cal} parameters to be large: $\rho_{c_{100}^{EE}, c_{143}^{EE}} = 81\%$, $\rho_{c_{100}^{EE}, c_{217}^{EE}} = 60\%$ and $\rho_{c_{100}^{EE}, c_{143}^{EE}} = 66\%$. These correlations are then lifted when adding information from TT.

In terms of the impact on cosmological parameter constraints when allowing P_{cal} parameters to float, we show the fractional difference in ΛCDM parameter uncertainties in Fig. 7 for TE,EE and Fig. 8 for TT,TE,EE. Similar to what we see in SPTPOL, we observe negligible to mild degradation in ΛCDM parameter uncertainties besides those for $\ln(10^{10}A_s)$, given the correlations between the P_{cal} parameters and $\ln(10^{10}A_s)$. For the TE,EE data set, the uncertainty of $\ln(10^{10}A_s)$ increases by $\sim 20\%$ when the P_{cal} parameters are allowed to float. Once TT is included, which independently constrains $\ln(10^{10}A_s)$, we see that floating P_{cal} has negligible impact on all ΛCDM parameters. We will see similar trends in our forecasts in Sec. VI.

C. Extended models

We now turn to extensions to the ΛCDM model. Similar to Sec. III, we check the constraints on P_{cal} for three extensions, A_L , Σm_ν , and N_{eff} . The P_{cal} uncertainties are shown in Fig. 5 for TE,EE and TT,TE,EE. We see that in all cases, the uncertainties of the P_{cal} parameters are similar to those in ΛCDM . As for the cosmological parameter uncertainties, Figures 7 and 8 show the increase in their error bars when marginalizing over polarization calibration parameters for *Planck* TE,EE and TT,TE,EE respectively.

The parameter uncertainties in $\Lambda\text{CDM}+N_{\text{eff}}$ are little affected, with increases in the error bars by less than 15%. On the contrary, we find a somewhat larger effect on parameter uncertainties in the $\Lambda\text{CDM}+\Sigma m_\nu$ model for the TE,EE data. In this case, marginalizing over P_{cal} increases the upper limit on Σm_ν by almost 40%, while degrading the uncertainties on H_0 and σ_8 by almost 30%. We note that the main source causing the degradation in Σm_ν does not come from a drastic increase in posterior uncertainty given the degeneracy between Σm_ν and P_{cal} . The main effect rather comes from a shift in the best-fit values of correlated parameters Σm_ν , $\ln(10^{10}A_s)$, and P_{cal} . For this data set, TE dominates the fit and causes Σm_ν and $\ln(10^{10}A_s)$ to be anti-correlated. With P_{cal} free, the best fit for $\ln(10^{10}A_s)$ shifts to lower values by about 0.7σ . Thus, a lower value of $\ln(10^{10}A_s)$ induces a shift of the Σm_ν posterior distribution to higher values. Since this distribution is single-tailed with $\Sigma m_\nu > 0$, this shift is perceived as a change in the upper bounds. These degradations disappear once the TT data is included, because TT strongly constrains $\ln(10^{10}A_s)$. While

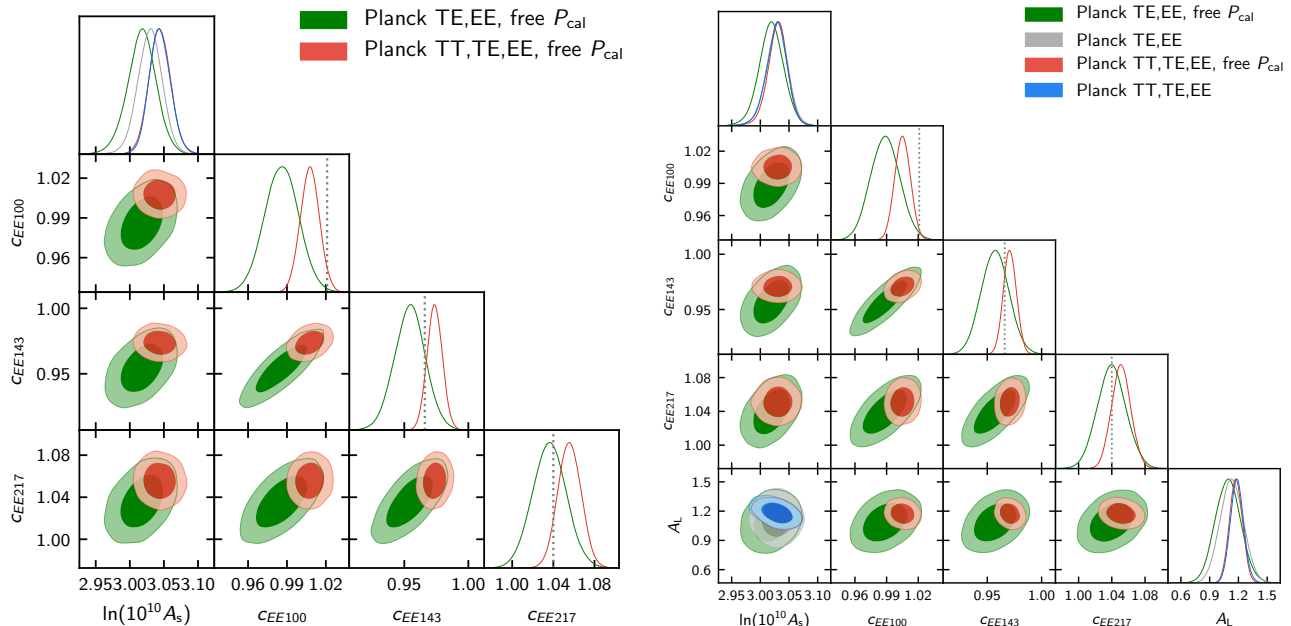


FIG. 6. One- and two-dimensional posterior distributions of the polarization efficiency parameters and cosmological parameters for *Planck* TE,EE. The left panel shows the results for the Λ CDM model, while the right panel shows results for the Λ CDM+ A_L model.

this shift could be due to either a statistical fluctuation or a systematic error, it highlights the impact of P_{cal} on constraining $\sum m_\nu$.

For the Λ CDM+ A_L model, it was noted in *Planck* that the A_L parameter is high compared to the Λ CDM expectation—at the 2.8σ or 2.1σ levels⁶ for polarization calibrations estimated using *Planck*'s baseline or estimated using separate fits of TE and EE respectively, as already described above in Sec. V A. Here we show that leaving the polarization calibrations free to vary cannot alleviate the difference between these two results. This is due to the fact that the difference between the two *Planck* estimates of polarization efficiency from TE alone or from EE alone ($\Delta P_{\text{cal}} \sim 0.017$ at 143 GHz at map level) is larger than the P_{cal} posterior width when P_{cal} is free to vary when fitting the TE,EE or TT,TE,EE data ($\sigma(P_{\text{cal}}) \lesssim 0.01$). Furthermore, the P_{cal} mean values measured from these fits are in good agreement with those of the baseline estimates.⁷ Therefore, leaving P_{cal} free to vary provides results which are similar to the baseline case. Specifically, using the TE,EE+lowE data set, the A_L parameter best fit is $A_L = 1.09 \pm 0.13$, which is within $0.8\sigma_{\text{exp}}$ of the value obtained when fixing P_{cal} in the baseline case, $A_L = 1.13 \pm 0.12$, with negligible impact on the uncertainties. Similarly when

also including TT, varying the polarization calibrations leads to $A_L = 1.19 \pm 0.069$, in agreement with the baseline result obtained with P_{cal} fixed $A_L = 1.18 \pm 0.068$ (see also the discussion in section 3.7 of [7]). Thus, leaving the polarization calibrations free to vary has a very small impact on the value and error bar of the A_L parameter, which remains higher than unity at the 2.8σ level, due to the tight constraint provided by the TE,EE or TT,TE,EE data combinations which agree with the baseline estimate. For the same reason, the other cosmological parameters are little affected as well.

VI. FORECASTS

In this section, we forecast how well P_{cal} could be measured with our method and the impact on cosmological parameter uncertainties when marginalizing over P_{cal} for ongoing and future experiments. We consider two experiment configurations: SPT-3G, the third-generation camera currently installed on the South Pole Telescope [13, 30], and CMB-S4, a next-generation ground-based CMB experiment [17].

A. SPT-3G

The SPT-3G receiver observes in three frequency bands 95, 150, and 220 GHz in both intensity and polarization with ~ 16000 detectors over ~ 1500 deg² of the sky in its main survey field. The full-width half-maximum of the beams are approximately 1.7, 1.2, and 1.1 arcminutes at 95, 150, and 220 GHz respectively. The first science results from SPT-

⁶These results refer to the baseline data combination TT,TE,EE+lowE+CMB lensing. Note that the A_L parameter only impacts the amplitude of lensing in the TT,TE,EE power spectra, while it leaves the *Planck* CMB lensing reconstruction power spectrum unaltered.

⁷This is not surprising since the P_{cal} fits obtained from the TE,EE or TT,TE,EE data are dominated by EE, which is also the data set used for the baseline estimates.

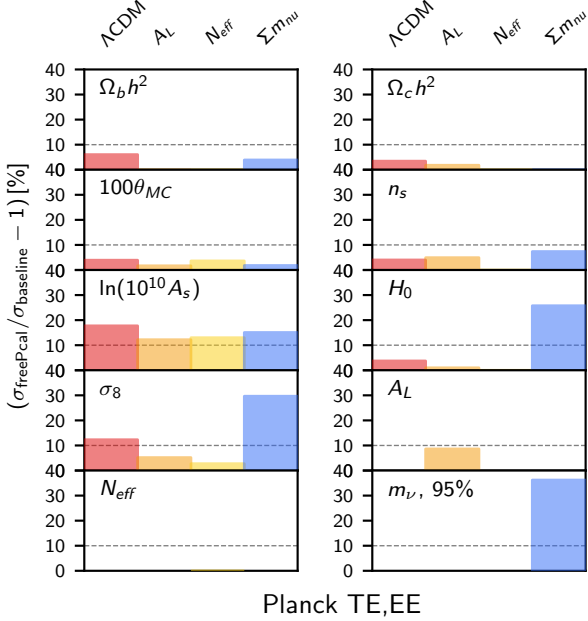


FIG. 7. Same as Figure 3, but for the *Planck* TE,EE data. Freeing the *Planck* P_{cal} parameters for this data combination has a large impact only in the $\Lambda\text{CDM} + \Sigma m_\nu$ case, where the 95% confidence level upper limit on the sum of neutrino masses Σm_ν , and the error bars on derived parameters H_0 and σ_8 are increased by 30 – 40%. This is due to a shift in the best fit values of $\ln(10^{10} A_s)$, rather than an increase in degeneracies between parameters, see Sec. V C.

3G using TE and EE spectra measured using data collected in 2018 have recently been released [23]. However, the data were only collected for half of the observing season with part of the focal plane operable. Therefore, for this forecast, we use noise level projections starting from 2019 when the active detector count nearly doubled. With five seasons of observations on the main survey field (2019–2023 inclusive), the noise levels in the final coadded temperature maps are projected to be 3.0, 2.2, and 8.8 $\mu\text{K arcmin}$ in the three frequency bands, and those in the polarization maps are a factor of $\sqrt{2}$ higher [13, 30].

We forecast the P_{cal} constraints along with constraints on ΛCDM and extension parameters for SPT-3G for two scenarios. First, we use data from only one of the three frequency bands, 150GHz, for more direct comparison with SPTPOL, described in Sec. III, and to verify the impact of using only one frequency channel. Second, we report the constraints when combining maps from all three bands.

We use the Fisher Matrix formalism and code described in [6] for extracting the $1-\sigma$ parameter uncertainties. As inputs, we use lensed power spectra of TT, TE, and EE; we do not include the lensing reconstruction spectrum $C_L^{\phi\phi}$. We present constraints from the combination of TE and EE as a baseline and also those including all three spectra to study the effect of including TT. We restrict the power spectrum angular

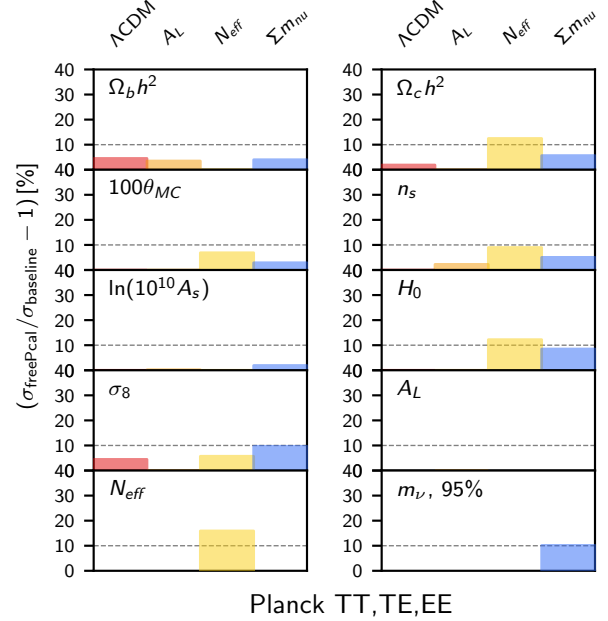


FIG. 8. Same as Figure 3, but for the *Planck* TT,TE,EE data. Freeing the three *Planck* P_{cal} frequency parameters has a very minor impact on the cosmological parameter error bars, smaller than 15%, in all the cosmological models considered here.

multipole range to $\ell = 100 - 3500$, and we adopt a Gaussian prior on the optical depth to reionization of $\sigma(\tau) = 0.007$, based on the *Planck* constraint [24]. We check that including $1/f$ noise or marginalizing over foregrounds do not change these results substantially.

Table III shows results for the ΛCDM case. The SPT-3G TE and EE combination is projected to constrain P_{cal} at the level of $\sim 0.8\%$, either using only one frequency or combining the information from all three frequencies. When freeing P_{cal} , the constraint on $\ln(10^{10} A_s)$ is degraded by about 50% while the rest of the ΛCDM parameters are mildly affected (below the 15% level). Similar to what is seen in the *Planck* case, the degraded constraints can be recovered by adding the TT data. In this case, marginalizing over P_{cal} has negligible impact on cosmological parameters and the constraint on P_{cal} tightens to 0.2%.

We verify that similar constraints on P_{cal} are obtained in extensions of the ΛCDM model, such as $\Lambda\text{CDM} + N_{\text{eff}}$, $\Lambda\text{CDM} + A_L$ or $\Lambda\text{CDM} + \Sigma m_\nu$, for both the TE+EE and the TT+TE+EE data combination. As for the cosmological parameters, we highlight here the ones with constraints degraded when marginalizing over P_{cal} . In $\Lambda\text{CDM} + \Sigma m_\nu$, the $\ln(10^{10} A_s)$ uncertainty increases by 40% for the TE+EE data combination. In $\Lambda\text{CDM} + N_{\text{eff}}$, the $\ln(10^{10} A_s)$ uncertainty increases by 70% and the uncertainties on $\Omega_b h^2$ and H_0 increase by $\sim 30\%$. However, similar to the ΛCDM case, when including the TT data, the marginalization over P_{cal} has minimal impact on the constraints on cosmological parameters.

TABLE III. Fisher matrix forecast on cosmological parameters and P_{cal} for SPT-3G, using the 150 GHz channel alone or all of the three channels. As a comparison, we also show constraints when fixing P_{cal} .

	$\Omega_b h^2$ [$\times 10^{-4}$]	$\Omega_c h^2$ [$\times 10^{-3}$]	H_0 [$\times 10^{-1}$]	τ [$\times 10^{-3}$]	ns [$\times 10^{-3}$]	$\ln[10^{10} A_s]$ [$\times 10^{-2}$]	P_{cal} [$\times 10^{-3}$]
ΛCDM							
SPT-3G TE+EE 150GHz	1.4	2.0	7.5	6.6	8.0	1.3	
SPT-3G TE+EE	1.3	1.9	7.1	6.6	7.7	1.3	
SPT-3G TT+TE+EE	1.4	1.7	6.5	6.4	7.4	1.2	
$\Lambda\text{CDM}+P_{\text{cal}}$							
SPT-3G TE+EE 150GHz	1.6	2.1	8.0	6.6	8.2	2.0	7.6
SPT-3G TE+EE	1.5	2.0	7.7	6.6	7.9	1.9	7.4
SPT-3G TT+TE+EE	1.4	1.8	6.8	6.4	7.4	1.2	2.1

B. CMB-S4

CMB-S4 is a next-generation ground-based CMB experiment aiming to observe $\sim 70\%$ of the sky. It is planned to have a frequency coverage from 20 to 270 GHz and the full-width half-maximum of its beam at 150 GHz is $\lesssim 1.5$ arcminutes [17]. There will be telescopes observing from both the South Pole and from the Atacama desert in Chile, for a deep and a wide area survey respectively.

In this work, we forecast the constraints on P_{cal} given the wide survey from Chile. We use noise curves from [31], which combine information from all frequencies using an internal linear combination method. The per-frequency noise input includes atmospheric noise; the output noise curves include residuals from component separation. We assume $f_{\text{sky}} = 0.42$, which excludes the area covering the galaxy in the wide survey. As in the forecast for SPT-3G, we use lensed power spectra in the multipole range of $\ell = 100 - 3500$ and we do not include information from lensing reconstruction $C_L^{\phi\phi}$.

Table IV shows results for the ΛCDM case. We find that with just TE and EE, CMB-S4 data could constrain P_{cal} at the level of $\sim 0.2\%$, which further tightens to 0.056% when we add TT. When freeing P_{cal} , constraints on cosmological parameters are mildly degraded without TT, and negligibly degraded with TT. As in the previous sections, we verify that extending the ΛCDM model with $\sum m_\nu$, N_{eff} , and A_L does not significantly change the constraints on P_{cal} . Conversely, leaving the P_{cal} parameter free has the largest impact on the constraints on $\Omega_b h^2$, H_0 and $\ln(10^{10} A_s)$ in the $\Lambda\text{CDM}+N_{\text{eff}}$ model for TE+EE, at the level of 30%. Similarly to previous cases, including the TT data allows us to marginalize over P_{cal} with no loss of precision on cosmological parameters.

VII. CONCLUSIONS

In this paper, we demonstrate that effective polarization calibrations P_{cal} could be precisely determined by fitting CMB TE and EE spectra to the ΛCDM model and its common extensions with P_{cal} as a free parameter. This is possible thanks to the different dependence of the TE and EE spectra on P_{cal} . While allowing P_{cal} to float does increase the posterior volume and therefore degrades some constraints on cosmological

parameters, we show that the degradation becomes negligible once TT is included.

We apply the method to SPT_{POL} and *Planck*. For the SPT_{POL} 150 GHz TE and EE data set presented in H18, we extract P_{cal} with an uncertainty of $\sim 2\%$ at the map level, independent of the considered models. For the data set from the *Planck* 2018 data release, combining TE and EE allows us to measure P_{cal} at 100, 143, and 217 GHz with uncertainties of 0.7%, 0.6% and 0.8% at the map level. We highlight how this method can be useful for detecting inconsistencies in the data. In particular, P_{cal} determined using TE and EE should agree with the ones determined with TT included or the ones measured from external data sets. If not, this could suggest the existence of unaccounted for systematics which project into these multiplicative factors.

Finally, we forecast the capabilities of current and future experiments to constrain P_{cal} . We find that using its 3 frequency channels, SPT-3G will be able to measure P_{cal} with an uncertainty of 0.7% from TE and EE, and the uncertainty can be improved to 0.2% when including TT. We find that leaving P_{cal} free to vary will degrade the constraints on A_s from TE and EE by 30%, while constraints from TT,TE,EE are not affected. Furthermore, we find that CMB-S4 could further tighten the uncertainty of P_{cal} to 0.2% with its TE and EE measurements and to 0.06% with TT,TE,EE. Similarly to SPT-3G, while constraints on A_s are affected by the variation of P_{cal} by about 20% when using TE,EE, the constraints from TT,TE,EE are unaffected.

We highlight that these uncertainties on P_{cal} are comparable to or tighter than those derived for the *Planck* baseline ($\sim 0.5\%$). As a consequence, relying on *Planck* to calibrate polarization maps will ultimately limit the accuracy of these experiments, provided that the *Planck* uncertainty is folded in the power spectrum covariance matrix. Furthermore, if the external P_{cal} determination is biased and the systematic uncertainties are not properly included, cosmological parameters constraints would be biased. We observe a possible hint of this in the *Planck* TE,EE $\sum m_\nu$ upper limits between the (baseline) fixed P_{cal} case and the free P_{cal} case. For *Planck* however, the difference of $\sum m_\nu$ upper limits due to a shift in the P_{cal} values is still compatible with a statistical fluctuation. For future experiments, we emphasize that stringent control on P_{cal} is important for accurate and precise inference on cosmological parameters, such as the sum of neutrino masses.

TABLE IV. Fisher matrix forecast on cosmological parameters and P_{cal} for CMB-S4. As a comparison, we also show constraints when not varying the P_{cal} .

	$\Omega_b h^2$ [$\times 10^{-4}$]	$\Omega_c h^2$ [$\times 10^{-3}$]	H_0 [$\times 10^{-1}$]	τ [$\times 10^{-3}$]	ns [$\times 10^{-3}$]	$\ln[10^{10} A_s]$ [$\times 10^{-2}$]	P_{cal} [$\times 10^{-3}$]
ΛCDM							
CMB-S4 TE+EE	0.36	0.71	2.7	5.1	2.5	0.88	
CMB-S4 TT+TE+EE	0.36	0.67	2.5	4.9	2.3	0.85	
$\Lambda\text{CDM}+P_{\text{cal}}$							
CMB-S4 TE+EE	0.42	0.75	2.9	5.1	2.5	1.0	2.0
CMB-S4 TT+TE+EE	0.37	0.70	2.6	4.9	2.3	0.86	0.56

Beyond using the primary CMB spectra TT, TE, and EE, we acknowledge the possibility of adding lensing potential power spectrum measurements to further tighten constraints on P_{cal} and reduce degradations in cosmological parameters. We leave this for future work. In conclusion, this paper demonstrates that a significant source of systematic error for future CMB polarization experiments can be self-calibrated without major consequences on the constraints on cosmological parameters.

ACKNOWLEDGMENTS

We thank the participants of the CMB systematics and calibration focus workshop hosted virtually by Kavli IPMU for

helpful comments and feedback. This work was completed in part with resources provided by the University of Chicago's Research Computing Center. This work has received funding from the French Centre National d'Etudes Spatiales (CNES). This research used resources of the IN2P3 Computer Center (<http://cc.in2p3.fr>). WLKW is supported in part by the Kavli Institute for Cosmological Physics at the University of Chicago through grant NSF PHY-1125897, an endowment from the Kavli Foundation and its founder Fred Kavli, and by the Department of Energy, Laboratory Directed Research and Development program and as part of the Panofsky Fellowship program at SLAC National Accelerator Laboratory, under contract DE-AC02-76SF00515. TC is supported by the the National Science Foundation through South Pole Telescope grant OPP-1852617.

-
- [1] C. Bennett et al. (WMAP), *Astrophys. J. Suppl.* **208**, 20 (2013), [arXiv:1212.5225](https://arxiv.org/abs/1212.5225) [astro-ph.CO].
- [2] N. Aghanim et al. (Planck), *Astron. Astrophys.* **607**, A95 (2017), [arXiv:1608.02487](https://arxiv.org/abs/1608.02487) [astro-ph.CO].
- [3] Y. Akrami et al. (Planck), (2018), [arXiv:1807.06205](https://arxiv.org/abs/1807.06205) [astro-ph.CO].
- [4] T. Louis et al. (ACTPol), *JCAP* **06**, 031 (2017), [arXiv:1610.02360](https://arxiv.org/abs/1610.02360) [astro-ph.CO].
- [5] K. Story et al. (SPT), *Astrophys. J.* **779**, 86 (2013), [arXiv:1210.7231](https://arxiv.org/abs/1210.7231) [astro-ph.CO].
- [6] S. Galli, K. Benabed, F. Bouchet, J.-F. Cardoso, F. Elsner, E. Hivon, A. Mangilli, S. Prunet, and B. Wandelt, *Phys. Rev. D* **90**, 063504 (2014), [arXiv:1403.5271](https://arxiv.org/abs/1403.5271) [astro-ph.CO].
- [7] N. Aghanim et al. (Planck), *Astron. Astrophys.* **641** (2020), [10.1051/0004-6361/201936386](https://arxiv.org/abs/10.1051/0004-6361/201936386), [arXiv:1907.12875](https://arxiv.org/abs/1907.12875) [astro-ph.CO].
- [8] N. Aghanim et al. (Planck), *Astron. Astrophys.* **641** (2020), [10.1051/0004-6361/201833910](https://arxiv.org/abs/10.1051/0004-6361/201833910), [arXiv:1807.06209](https://arxiv.org/abs/1807.06209) [astro-ph.CO].
- [9] N. Aghanim et al. (Planck), (2018), [arXiv:1807.06207](https://arxiv.org/abs/1807.06207) [astro-ph.CO].
- [10] Y. D. Takahashi, P. A. R. Ade, D. Barkats, J. O. Battle, E. M. Bierman, J. J. Bock, H. C. Chiang, C. D. Dowell, L. Duband, E. F. Hivon, W. L. Holzapfel, V. V. Hristov, W. C. Jones, B. G. Keating, J. M. Kovac, C. L. Kuo, A. E. Lange, E. M. Leitch, P. V. Mason, T. Matsumura, H. T. Nguyen, N. Ponthieu, C. Pryke, S. Richter, G. Rocha, and K. W. Yoon, *ApJ* **711**, 1141 (2010), [arXiv:0906.4069](https://arxiv.org/abs/0906.4069) [astro-ph.CO].
- [11] B. Koopman et al., *Proc. SPIE Int. Soc. Opt. Eng.* **9914**, 99142T (2016), [arXiv:1607.01825](https://arxiv.org/abs/1607.01825) [astro-ph.IM].
- [12] F. Nati, M. J. Devlin, M. Gerbino, B. R. Johnson, B. Keating, L. Pagano, and G. Teply, *J. Astron. Inst.* **06**, 1740008 (2017), [arXiv:1704.02704](https://arxiv.org/abs/1704.02704) [astro-ph.IM].
- [13] A. N. Bender et al., *Proc. SPIE Int. Soc. Opt. Eng.* **10708**, 1070803 (2018), [arXiv:1809.00036](https://arxiv.org/abs/1809.00036) [astro-ph.IM].
- [14] Y. Inoue et al. (POLARBEAR), *Proc. SPIE Int. Soc. Opt. Eng.* **9914**, 99141I (2016), [arXiv:1608.03025](https://arxiv.org/abs/1608.03025) [astro-ph.IM].
- [15] S. M. Simon et al., *Journal of Low Temperature Physics* **193**, 1041 (2018).
- [16] P. Ade et al. (Simons Observatory), *JCAP* **02**, 056 (2019), [arXiv:1808.07445](https://arxiv.org/abs/1808.07445) [astro-ph.CO].
- [17] K. Abazajian et al., (2019), [arXiv:1907.04473](https://arxiv.org/abs/1907.04473) [astro-ph.IM].
- [18] J. Henning et al. (SPT), *Astrophys. J.* **852**, 97 (2018), [arXiv:1707.09353](https://arxiv.org/abs/1707.09353) [astro-ph.CO].
- [19] N. Aghanim et al. (Planck), *Astron. Astrophys.* **641** (2020), [10.1051/0004-6361/201833880](https://arxiv.org/abs/10.1051/0004-6361/201833880).
- [20] S. Aiola et al. (ACT), (2020), [arXiv:2007.07288](https://arxiv.org/abs/2007.07288) [astro-ph.CO].
- [21] A. Lewis and S. Bridle, *Phys. Rev. D* **66**, 103511 (2002), [arXiv:astro-ph/0205436](https://arxiv.org/abs/astro-ph/0205436) [astro-ph].
- [22] J. Torrado and A. Lewis, *arXiv e-prints*, [arXiv:2005.05290](https://arxiv.org/abs/2005.05290) (2020), [arXiv:2005.05290](https://arxiv.org/abs/2005.05290) [astro-ph.IM].
- [23] D. Dutcher et al. (SPT-3G), (2021), [arXiv:2101.01684](https://arxiv.org/abs/2101.01684) [astro-ph.CO].
- [24] N. Aghanim et al. (Planck), (2018), [arXiv:1807.06209](https://arxiv.org/abs/1807.06209) [astro-ph.CO].
- [25] A. Manzotti, W. Hu, and A. Benoit-Lévy, *Phys. Rev. D* **90**, 023003 (2014), [arXiv:1401.7992](https://arxiv.org/abs/1401.7992) [astro-ph.CO].
- [26] E. Calabrese, A. Slosar, A. r. Melchiorri, G. F. Smoot, and

- O. Zahn, *Phys. Rev. D* **77**, 123531 (2008), [arXiv:0803.2309 \[astro-ph\]](#).
- [27] S. K. Choi *et al.* (ACT), *JCAP* **12**, 045 (2020), [arXiv:2007.07289 \[astro-ph.CO\]](#).
- [28] C. Rosset *et al.*, *A&A* **520**, A13 (2010), [arXiv:1004.2595 \[astro-ph.CO\]](#).
- [29] S. Gratton and A. Challinor, arXiv e-prints, [arXiv:1911.07754 \(2019\)](#), [arXiv:1911.07754 \[astro-ph.IM\]](#).
- [30] B. Benson *et al.* (SPT-3G), *Proc. SPIE Int. Soc. Opt. Eng.* **9153**, 91531P (2014), [arXiv:1407.2973 \[astro-ph.IM\]](#).
- [31] https://cmb-s4.org/wiki/index.php/Survey_Performance_Expectations.